GEOPHYSICAL RESEARCH LETTERS, VOL. 33, L20303, doi:10.1029/2006GL027957, 2006

Click Here for Full Article

Using satellite data to characterize the temporal thermal behavior of an active volcano: Mount St. Helens, WA

R. Greg Vaughan[1] and Simon J. Hook[1]

Received 25 August 2006; accepted 13 September 2006; published 17 October 2006.

[1] ASTER thermal infrared data over Mt. St Helens were used to characterize its thermal behavior from Jun 2000 to Feb 2006. Prior to the Oct 2004 eruption, the average crater temperature varied seasonally between −12 and 6 C. After the eruption, maximum single-pixel temperature increased from 10 C (Oct 2004) to 96 C (Aug 2005), then showed a decrease to Feb 2006. The initial increase in temperature was correlated with dome morphology and growth rate and the subsequent decrease was interpreted to relate to both seasonal trends and a decreased growth rate/increased cooling rate, possibly suggesting a significant change in the volcanic system. A single-pixel ASTER thermal anomaly first appeared on Oct 1, 2004, eleven hours after the first eruption - 10 days before new lava was exposed at the surface. By contrast, an automated algorithm for detecting thermal anomalies in MODIS data did not trigger an alert until Dec 18. However, a single-pixel thermal anomaly first appeared in MODIS channel 23 (4 um) on Oct 13, 12 days after the first eruption - 2 days after lava was exposed. The earlier thermal anomaly detected with ASTER data is attributed to the higher spatial resolution (90 m) compared with MODIS (1 km) and the earlier visual observation of anomalous pixels compared to the automated detection method suggests that local spatial statistics and background radiance data could improve automated detection methods. **Citation:** Vaughan, R. G., and S. J. Hook (2006), Using satellite data to characterize the temporal thermal behavior of an active volcano: Mount St. Helens, WA, *Geophys. Res. Lett.*, *33*, L20303, doi:10.1029/2006GL027957.

1. Introduction

[2] Immediately following most volcanic eruptions there are numerous features that can be identified based on their thermal characteristics (e.g. lava/pyroclastic flows, lava lakes, domes, crater lakes and fumaroles). Thermal surface expressions of volcanic activity can be detected remotely for continual monitoring and, if detected before an eruption, potentially used for prediction [*Pieri and Abrams*, 2005]. As a result, satellite and airborne remote sensing observations have been used for many years to study volcanic thermal features [*Francis and Rothery*, 1987; *Oppenheimer et al.*, 1993; *Wooster and Kaneko*, 1998; *Harris et al.*, 2002; *Wright et al.*, 2004; *Ramsey and Dehn*, 2004; *Vaughan et al.*, 2005].

[3] In Sept 2004 Mount St Helens (MSH) (Figure 1) reawakened with a swarm of shallow earthquakes followed within days by surface bulging and a series of phreatic eruptions on Oct 1–5. Fresh lava first extruded onto the surface on Oct 11 as a spine of solid, but still hot (~620 C) dacite lava [*Dzurisin et al.*, 2005; *Major et al.*, 2005; *Vaughan et al.*, 2005]. In the following months a series of larger lobes of solid lava extruded, broke apart into rubble, and were pushed aside by new lobes, continually increasing the dome volume [*Vallance et al.*, 2005; *Dzurisin et al.*, 2005; *Major et al.*, 2005]. As of Apr 2006 the new dome had reached a volume of 81 million m^3 and continues to grow as of this writing (see http://vulcan.wr.usgs.gov) (Figure 1).

[4] To quantify the pre-eruption range of dome temperatures and characterize the thermal behavior of the dome since the 2004 eruption began, Advanced Spaceborne Thermal Emission and Reflection Radiometer (ASTER) data collected between Jun 2000 and Feb 2006 were analyzed and used to extract surface temperatures. Thirty-five cloud-free ASTER scenes were acquired over MSH during this time frame, 20 of which were nighttime scenes. The TIR data were visually scrutinized to determine if any clouds or plume material could interfere with dome-emitted radiance and only totally clear scenes were used. Also, to eliminate solar reflected radiance contribution only the nighttime scenes were used. The objectives were to, 1) develop a baseline for the thermal behavior of the volcanic dome at MSH by characterizing the pre-eruption background temperature variations measured by ASTER, 2) identify how temporal changes in ASTER-derived temperatures may correlate to dome growth processes, and 3) determine when and why, the first thermal anomaly indicative of renewed activity was detected by ASTER, which may help improve remote thermal anomaly detection. Because thermal anomaly detection is strongly dependent on both spatial and temporal resolution, ASTER data were also compared to data from the Moderate Resolution Imaging Spectrometer (MODIS), another satellite instrument with lower (1-km) spatial resolution in the TIR but more frequent (daily) coverage of MSH [*Salomonson et al.*, 1989].

2. Physical Basis

[5] Spaceborne land-imaging visible-infrared sensors typically measure the energy reflected or emitted from the surface in three broad spectral regions that are least affected by atmospheric effects. These atmospheric window regions are in the visible, near-infrared/shortwave infrared (VNIR/SWIR; 0.4–2.5 um), mid infrared (MIR; 3–5 um) and thermal infrared (TIR; 7–14 um). The radiance emitted from a surface is a function of its temperature and emissivity and for surfaces at typical terrestrial temperatures (<80 C)

[1]Jet Propulsion Laboratory, Pasadena, California, USA.

0094-8276/06/2006GL027957$05.00

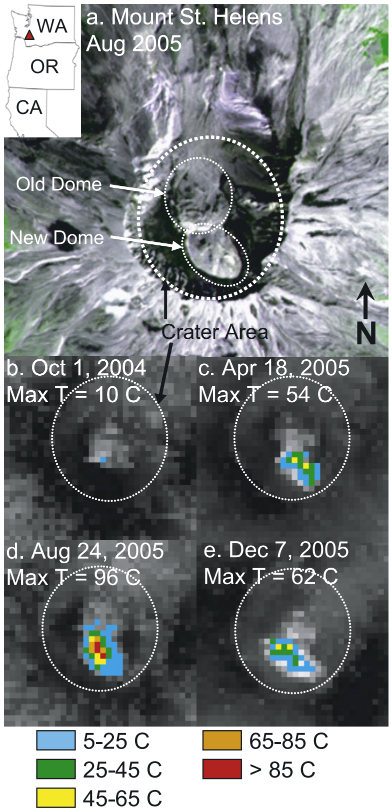

Figure 1. Mount St. Helens location. (a) Daytime visible image from Aug 2005. ASTER TIR temperature images from (b) Oct 1, 2004, (c) Apr 18, 2005, (d) Aug 24, 2005, and (e) Dec 7, 2005. In the grey-scale temperature images, temperatures (TES-derived, PIT) on the new dome (south of the old dome) that are >5 C are mapped in color (see legend). The large circular area (dotted line) in each image is approximately 2 km in diameter and represents the crater area over which temperature data were averaged.

the emitted radiance can only be detected in the MIR and TIR regions. During the day there is an additional contribution from reflected solar energy in the VNIR/SWIR and MIR. The MODIS instrument measures radiance from the surface in the VNIR/SWIR, MIR and TIR whereas the ASTER instrument measures radiance from the surface in the VNIR/SWIR and TIR. For any given temperature, spectral radiance is defined by the Planck function and the peak emitted radiance shifts to shorter wavelengths with increasing temperature [e.g., *Rothery et al.*, 1988]. Thus, at higher temperatures (100–1000 C) typical of active volcanic features, emitted radiance can also be measured with MIR and VNIR/SWIR wavelength channels.

[6] Hot volcanic features are typically smaller in spatial extent than the area covered by ASTER's 90-m pixels. As a result, the radiance measured is a pixel-integrated radiance that is an area-weighted sum of multiple sub-pixel radiating components. Temperature derived from radiance data, whether by inversion of the Planck function or by temperature-emissivity separation (TES), is therefore a pixel-integrated temperature (PIT). Both the ASTER and MODIS surface temperature data were derived using a MODTRAN-based atmospheric correction and the TES method described by *Gillespie et al.* [1998], and are provided as validated data products. ASTER TIR data saturate above radiance values that correspond to a brightness temperature of ~97 C; thus far only one saturated pixel has been observed on one date in one channel (8-24-2005, channel 10). Data integrity tests in the TES algorithm eliminate this pixel from the calculations, which slightly lowers the crater-averaged temperature retrieved for that date.

[7] In this study, we focus on TES-derived temperatures and relate temperature changes to both seasonal and volcanic dome growth processes. The potential for using ASTER's 5 TIR channels together with the 6 higher-resolution SWIR channels to test our hypotheses and for sub-pixel temperature component modeling will be relegated to future work.

3. Instrument Summaries

[8] The ASTER and MODIS instruments are mounted on the Terra spacecraft which was launched in 1999. The ASTER instrument measures radiance in 14 spectral channels from the visible through the TIR region [*Yamaguchi et al.*, 1998]. The 5 TIR channels (10–14) acquire data between 8.2 and 11.3 μm, have 90-m spatial resolution, and were used to extract temperature information in this study. MODIS acquires radiance data in 36 spectral channels. Channels 20–25 cover the MIR region and are used in conjunction with the TIR measurements (channels 29–36) to detect thermal anomalies using a normalized thermal index [*Wright et al.*, 2004]. All of the MODIS MIR and TIR channels have a 1-km spatial resolution [*Salomonson et al.*, 1989].

4. Results and Interpretation

[9] ASTER data for the 20 nighttime scenes over the last 5 years show that pre-eruption temperatures averaged over the MSH crater (see Figure 1e) ranged from −12 to 6 C; maximum single-pixel temperatures ranged from −8 to 15 C (Figure 2). Post-eruption average temperatures ranged from −10 to 8 C; maximum single-pixel temperatures

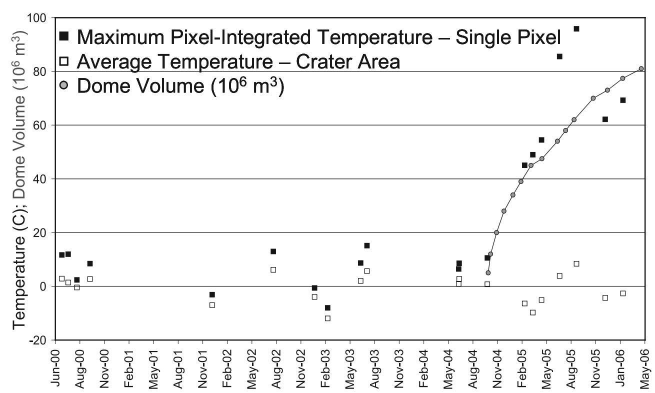

Figure 2. Plot of ASTER-derived temperatures vs. date over the last 5 years. Open squares are temperatures (TES-derived, PIT) averaged over the dome area; black squares are maximum single-pixel temperatures (TES-derived, PIT); circles are dome volume estimates from the USGS CVO.

ranged from 10 to 96 C. The crater-averaged temperatures varied in conjunction with the seasons, even after the eruption, and suggest that varying amounts of snow/ice cover dominate the measured TIR radiance averaged over that area ($\sim$3 km^2). The maximum single-pixel temperatures also correlate with seasonal trends before the eruption, but increase noticeably afterwards. The post-eruption increase in maximum temperatures can be interpreted as either, 1) increasing temperatures, or 2) increasing sub-pixel areas of static high temperatures. Independent temperature measurements made by the USGS between Oct 2004 and Sept 2005 of exposed, fresh (solid, but still very hot) dacite lava consistently recorded high temperatures around 600 C (R. Wessels, personal communication, 2005). Therefore we favor the latter interpretation, which reflects a growing dome dominated by areas at near-ambient background temperature but with increasing areas of either exposed fresh lava or freshly exposed hot rock from rock falls.

[10] The lava that formed the new dome extruded as solid lobes with smooth surfaces covered with fine-grained fault gouge that cooled very quickly to near-ambient temperatures [*Vallance et al.*, 2005]. In general, the hottest areas were observed near fumaroles and in areas of recent rock collapse and fractures that expose hotter underlying rock [*Dzurisin et al.*, 2005]. The initial positive correlation between the maximum temperature increase and dome volume was interpreted to relate to this phase of extrusive dome growth. In Apr 2005 smooth lobe surfaces largely collapsed into rubble piles during an interval between different lobe extrusions (based on high-resolution photographs of the dome courtesy of the USGS Cascades Volcano Observatory) and eruption chronology reports (http://vulcan.wr.usgs.gov/Volcanoes/MSH). This change in the morphology of the dome could have resulted in a more even distribution of high temperatures across the dome and thus an increase in TES-derived PIT. Although the frequency of ASTER data is too low to detect the temperature effects of daily rock falls that expose hotter lava, such dome building processes result in detectable increases in TIR radiance that can be monitored remotely.

[11] After the Aug 2005 temperature maximum, temperatures decreased (Figure 2). Because of the timing of this trend (high temperature in summer, lower temperature in winter), it appears to reflect a seasonal effect overprinted on volcanically elevated temperatures. Based on USGS photographs of the dome, there was increased snow cover over part of the dome in Dec, 2005, but the hottest areas appear to be snow-free, thus it is unlikely that the maximum single-pixel temperatures are influenced by partial snow cover. Although the temperature decrease after Aug 2005 may be partly related to seasonal effects, it may also indicate significant a change in overall dome growth processes. It could be related to a decrease in the growth rate, though this is not supported by the dome volume measurements, or more likely a decrease in the rate and/or size of new cracks and rock falls that expose hotter underlying rock. Also, the lower temperatures could be influenced by colder winter air temperatures in the layer just above the ground, increasing the radiative cooling rate. To test these hypotheses, it would be useful to analyze concurrent data on gas emissions and/or seismic activity. Regardless, such temporal thermal behavior is important to monitor as it could indicate a significant change in the behavior of the volcanic system preceding explosive activity. Also, it is important to understand how to interpret TIR-derived PIT for characterizing other volcanoes that are not as closely monitored as MSH.

[12] On Oct 1, 2004, eleven hours after the first phreatic eruption of steam and ash (10 days before lava came to the surface) ASTER 90-m TIR data detected a subtle single-pixel thermal anomaly based on visual image analysis (Figure 1b). The temperature for that pixel (10 C) was within the pre-eruption temperature range and thus could not be uniquely identified as a thermal anomaly via standard statistical analyses of the radiance or temperature data (e.g. data contrast, % difference, or standard deviation). This is a recognized limitation to the remote detection of subtle thermal anomalies that is particularly important for monitoring perennially snow/ice covered volcanoes [*Pieri and Abrams*, 2005].

[13] This problem of combining quantitative data analysis with automated recognition and interpretation of significant spatial patterns is also apparent in the MODIS thermal alert system. MODIS data are used to operate a global thermal anomaly alert system, which uses a ratio of MIR and TIR radiance data and a predefined threshold value for automated anomaly detection [*Wright et al.*, 2004]. Because of the frequent revisit time, MODIS is ideal for global monitoring. The low (1-km) spatial resolution trade-off for this high temporal coverage, combined with the threshold value required to minimize false anomalies, means that many small hot spots will go unnoticed. The MODIS system did not trigger a thermal anomaly alert at MSH until Dec 18, 2004. However, MODIS MIR data (channel 23; 4 um) detected a single-pixel thermal anomaly based on visual image analysis on Oct 13, 2004, two days after lava first broke the surface. The ability of satellite instruments to detect subtle thermal anomalies indicative of near-real time volcanic activity remains limited by both achievable spatial and temporal resolution and the challenge of automated data analysis without subjective human interpretation.

5. Summary and Conclusions

[14] Multispectral TIR ASTER data were used to measure surface temperatures inside the crater at MSH and relate changes in the temperatures to different phases of dome growth. Increasing temperatures measured by ASTER were correlative with dome growth during the period from Oct 2004 to Aug 2005. The initial increase in maximum single-pixel temperatures was due to initial dome extrusion and was approximately linearly correlated with dome volume increase. The more rapid temperature increase between April and Aug 2005 was possibly due to a change in the morphology of the dome from a smooth, fault-gouge-covered lobe with small high-temperature fractures, to a rough-textured rubble pile with increased area of high-temperature rocks. This hypothesis is supported by USGS CVO photo archive data. The decrease in the temperature after Aug 2005 may be due to a combination of seasonal effects and the dome surface becoming more rapidly cooled. Given that the dome volume continued to increase during that interval, this could suggest a significant change in volcanic processes such as a repressurizing of the volcanic system, or just a decrease in the rate/area of fractures and

rock falls. This pattern of temperature change, separated from natural seasonal variation, is an important characteristic to measure in remote volcano monitoring efforts.

[15] The ASTER data were also compared to MODIS data to illustrate the challenge of sub-pixel thermal anomaly detection at various scales. Eleven hours after the first phreatic eruption on Oct 1, 2004 both ASTER and MODIS acquired clear nighttime images over MSH. On this date, a subtle thermal anomaly was only observed in the ASTER image due to its higher spatial resolution. The ASTER-derived pixel temperature was within the range of pre-eruption temperatures observed in this study and thus could not have been uniquely identified without visual interpretation. This was also true for MODIS, which displayed a thermal anomaly in the MIR image data two months before the automated thermal alarm was triggered.

[16] This study identified a significant relationship between the changes in TES-derived PIT and the phases of lava dome growth and shows that a time-series analysis of ASTER-derived temperature data can be used to determine trends in the heating and radiative cooling of an active lava dome. This study also highlights the benefits that would be obtained from TIR data with higher temporal and spatial resolution. An ASTER-type instrument with higher temporal resolution could detect higher-frequency changes in dome growth and have a better chance of detecting thermal precursors to a volcanic eruption. Higher spatial resolution data could be used to determine the spatial distribution of hot fractures, rock falls, pyroclastic flows and other volcanic hazards [e.g., *Vaughan et al.*, 2005], and also used to uniquely detect sub-pixel thermal anomalies sooner and more accurately, allowing quicker response to global volcanic activity.

[17] Currently, ASTER represents the state-of-the-art in remote sensing instruments but future technological enhancements in terms of temporal, spatial and spectral resolution could all lead to considerable improvements in our ability to remotely monitor volcanic activity. At the present time there are no plans for an ASTER follow-on instrument and future Landsat instruments may not include any thermal channels. We hope studies such as this one will help justify the need for continued space-based thermal observations with instruments with a similar or greater number of thermal channels to ASTER.

[18] **Acknowledgments.** The research described in this paper was carried out in part at the Jet Propulsion Laboratory, California Institute of Technology, under a contract with NASA as part of the Earth Observing System Mission to Planet Earth Program. Work by R.G.V. was funded by a Caltech postdoctoral fellowship. Special thanks to Rick Wessels from the USGS AVO and to the USGS CVO for maintaining the excellent on-line documentation of the MSH eruption. Thanks also to Nina Potts, Dave Pieri, Mike Abrams, and Vince Realmuto at JPL. Thanks to 2 anonymous reviewers for providing some helpful comments on this manuscript. Reference herein to any specific commercial product, process, or service by trade names, trademark, manufacturer or otherwise does not imply endorsement by the United States or the Jet Propulsion Laboratory, California Institute of Technology.

References

Dzurisin, D., J. W. Vallance, T. M. Gerlach, S. C. Moran, and S. D. Malone (2005), Mount St. Helens reawakens, *Eos Trans. AGU*, *86*(3), 25–36.

Francis, P. W., and D. A. Rothery (1987), Using the Landsat thematic mapper to detect and monitor active volcanoes: An example from Lascar Volcano, northern Chile, *Geology*, *15*, 614–617.

Gillespie, A. R., S. Rokugawa, T. Matsunaga, J. S. Cothern, S. J. Hook, and A. B. Kahle (1998), A temperature and emissivity separation algorithm for Advanced Spaceborne Thermal Emission and Reflection Radiometer (ASTER) images, *IEEE Trans. Geosci. Remote Sens.*, *36*, 1113–1126.

Harris, A. J. L., L. P. Flynn, O. Matias, and W. I. Rose (2002), The thermal stealth flows of Santiaguito Dome, Guatemala: Implications for the cooling and emplacement of dacitic block-lava flows, *GSA Bull.*, *114*(5), 533–546.

Major, J. J., W. E. Scott, C. Driedger, and D. Dzurisin (2005), Mount St. Helens erupts again: Activity from September 2004 through March 2005, *U.S. Geol. Surv. Fact Sheet FS2005-3036*, 4 pp.

Oppenheimer, C., D. A. Rothery, and P. W. Francis (1993), Thermal distributions at Fumarole Fields: Implications for infrared remote sensing of active volcanoes, *J. Volcanol. Geotherm. Res.*, *55*, 97–115.

Pieri, D. C., and M. J. Abrams (2005), ASTER observations of thermal anomalies preceding the April 2003 eruption of Chikurachki Volcano, Kurile Islands, Russia, *Remote Sens. Environ.*, *99*, 84–94.

Ramsey, M. S., and J. Dehn (2004), Spaceborne observations of the 2000 Bezymianny, Kamchatka eruption: The integration of high-resolution ASTER data into near real-time monitoring using AVHRR, *J. Volcanol. Geotherm. Res.*, *135*, 127–146.

Rothery, D. A., P. W. Francis, and C. A. Wood (1988), Volcano monitoring using short wavelength infrared data from satellites, *J. Geophys. Res.*, *93*(B7), 7993–8008.

Salomonson, V., W. Barnes, P. Maymon, H. Montgomery, and H. Ostrow (1989), MODIS: Advanced facility instrument for studies of the Earth as a system, *IEEE Trans. Geosci. Remote Sens.*, *27*, 145–153.

Vallance, J. W., D. J. Schneider, M. Logan, and R. Wessels (2005), Evolution of dome growth at Mount St. Helens in 2004–2005: Airborne optical and thermal infrared observations, *Geol. Soc. Am. Abstr. Programs*, *37*(7), 531.

Vaughan, R. G., S. J. Hook, M. S. Ramsey, V. J. Realmuto, and D. J. Schneider (2005), Monitoring eruptive activity at Mount St. Helens with TIR image data, *Geophys. Res. Lett.*, *32*, L19305, doi:10.1029/2005GL024112.

Wooster, M. J., and T. Kaneko (1998), Satellite thermal analysis of lava dome effusion rates at Unzen Volcano, Japan, *J. Geophys. Res.*, *103*(B9), 20,935–20,947.

Wright, R., L. P. Flynn, H. Garbeil, A. J. L. Harris, and E. Pilger (2004), MODVOLC: Near-real-time thermal monitoring of global volcanism, *J. Volcanol. Geotherm. Res.*, *135*, 29–49.

Yamaguchi, Y., A. B. Kahle, H. Tsu, T. Kawakami, and M. Pniel (1998), Overview of Advanced Spaceborne Thermal Emission and Reflection Radiometer (ASTER), *IEEE Trans. Geosci. Remote Sens.*, *36*(4), 1062–1071.

S. J. Hook and R. G. Vaughan, Jet Propulsion Laboratory, MS 183-501, 4800 Oak Grove Dr., Pasadena, CA 91109, USA. (greg.vaughan@jpl.nasa.gov)